CITC GLOBAL
Construction in the 21st Century

The Fifteenth International Conference on Construction in the 21st Century (CITC-15)
Rabat, Morocco | November 10 - 14, 2025

Net-Zero by Retrofit: Data-Driven Construction Facilities Upgrades for Yarmouk University's Campus

Ali Shehadeh[1], Odey Alshboul[2], Ghassan Almasabha[3]

[1] Department of Civil Engineering, Hijjawi Faculty for Engineering Technology, Yarmouk University, P.O. Box 566, Irbid 21163, Jordan. (corresponding author). ali.shehadeh@yu.edu.jo
[2]Department of Civil Engineering, Faculty of Engineering, The Hashemite University, P.O. Box 330127, Zarqa 13133, Jordan. odey.shboul@hu.edu.jo
[3] Department of Civil Engineering, Faculty of Engineering, The Hashemite University, P.O. Box 330127, Zarqa 13133, Jordan. ghassans@hu.edu.jo

Abstract
This paper interprets Net Zero Energy Campus (NZEC) as a construction-oriented retrofit program to the teaching labs, workshops, and learning spaces of Yarmouk University. We leverage high-resolution power logs from the on-campus solar supervisory system to examine end-use patterns in construction-related spaces, relate loads to occupancy and weather conditions, and construct short-term forecasts (ARIMA/LSTM) to reveal avoidable peaks. We then assemble and evaluate sequenced energy conservation measures—HVAC right-sizing, envelope retrofits, variable-speed drives, advanced lighting, and controls—co-optimized with on-site PV and battery energy storage for peak shaving and self-consumption. Life-cycle cost and carbon screen prioritize measures, while construction management constraints (shutdown windows, phasing, and safety) are embedded so upgrades can be delivered with minimal disruption to teaching and research. The outcome is a tactical NZEC roadmap that couples' data analytics with buildable retrofit packages, procurement guidance, and measurement-and-verification protocols tailored to Jordan's climatic and regulatory context.

Keywords
construction facilities management; building retrofit; energy conservation measures; measurement and verification

1. Introduction

Achieving Net Zero Energy Campus (NZEC) status in higher education is often framed as a problem of new construction and showcase buildings (Feng et al., 2019); yet the dominant share of energy use, cost, and operational complexity sits within existing facilities. Teaching laboratories, workshops, and maker spaces relevant to and impacting construction-based activities at Yarmouk University have a distinct load profile characterized by the continual use of infra-structure being transient, 'high intensity' loads, and 'safety-forced' ventilation patterns. This profile complicates the use of existing playbooks that generally allow for application based on load profiles with reliable, plug and lighting loads or an office-type load schedule. Also, Jordan's climate and future energy typology: more evidence for solar resource expansion, broadening adoption of distributed PV technology, and the advent of 'dynamic tariffs' to better reflect energy peak demand - offers an extraordinary opportunity to provide demand reductions associated with production and storage on-site (Al-Oun et al., 2025; et al., Oduro et al., 2024). However, and at the same time, while much more attention is being drawn to Net Zero Energy Buildings (NZEB) within higher education systems, research shows there is still much work left to do to meet the aspirations and reality of sustainability (Jaysawal et al., 2022; Khemici et al., 2022). This inconsistency exists in even campus administration where dynamic complex projects with occupied facilities along with renewable technologies are under utilized (Jin & Bae, 2023; Parvin et al., 2022). It is this opportunity that was explored within the study under the planar of a retrofit planning

optimization exercise using data indicative of a construction-based approach as opposed to a traditional checklist of measures.

The central concept is that having high-resolution electrical data in addition to contextual signals (occupancy, weather, and academic schedules) will help to reveal preventable peaks, mis-sized HVAC, and controllable process loads that are otherwise hidden within the monthly billing statements. Power logs that can be mined from the campus's solar supervisory system, and contextualized with temperature, humidity, and usage patterns, may help disaggregate end uses and point to waste signatures: standby losses, coincident start-ups, and ventilation schedules that are not aligned with occupancy. Short-term forecasting models (ARIMA and LSTM) are then employed to quantify near-term demand trajectories to test and inform how sequencing measures, rescheduling activities, or shaping setpoints will subsequently impact peaks and energy use, all before any capital investment is committed. This predictive layer will be especially useful in workshop and lab-heavy contexts where compressed academic calendars and safety constraints hinder trial-and-error research.

Based on these analyses, we compile the ECMs appropriate to construction facilities: right-sizing and re-commissioning the make-up air and exhaustion systems; envelope and infiltration improvements in dust- and fume-managed areas; adding variable speed drives and soft-start control to mixers, saws, compressors and pumps; and smart lighting and occupancy control for high-bay areas. ECCMs are evaluated not in isolation but co-optimized with on-site photovoltaics (PV) and battery energy storage systems (BESS), as well as on-site use case to achieve priorities that support increasing self-consumption of PV outputs, peak shaving, and mitigating limits on grid connection. Life-Cycle Cost and Carbon screening incorporates initial capital costs, operation and maintenance, tariff conditions, and embodied impacts into a ranked portfolio that is both financially defensible and emissions-credible.

The roadmap incorporates realities of construction management. Upgrade packages will be grouped into buildable phases that align with semester breaks, lab downtimes, and safety considerations to minimize the impact on teaching and research. The procurement guidance has taken into consideration technical findings and translated them into specifications and contracting strategies appropriate for the context of Jordan's regulatory environment, and incorporates performance-based components and measurement-and-verification (M&V) plans that align with generally acceptable protocols. Additionally, because analytics and delivery discipline are coupled, the roadmap seeks to transition from a model to implementation without compromising fidelity (to cost, schedule remediations, or safety). This paper presents the following three advances. First, it presents a replicable methodology for end-use disaggregation and short-term forecasting; specifically tailored to workshop and lab environments. Second, it presents integrated ECM–PV–BESS optimization that provides value to operational flexibility alongside energy savings. Third, it provides a phasing and M&V framework that makes NZEC ambitions actionable within academic constraints. The remainder of the paper details the data sources and preprocessing; presents the forecasting and optimization models; reports retrofit portfolios, costs, and carbon outcomes; and discusses delivery phasing, procurement, and M&V considerations for campuswide scale-up.

2. Methods

This study develops a data-driven, construction-centric retrofit methodology that couples load analytics, short-term forecasting, and an integrated optimization of energy conservation measures (ECMs) with on-site photovoltaics (PV) and battery energy storage (BESS). The approach is applied to Yarmouk University's (YU) construction-related facilities (teaching labs, workshops, high-bay spaces) and benchmarked against a multi-institution dataset from U.S. construction facilities to inform transferability and parameter priors. The design is applied, quantitative, and quasi-experimental, using counterfactual simulation (pre/post retrofit portfolios) and measurement-and-verification (M&V) protocols. A computational design-science paradigm is adopted: (i) sense (data acquisition and QA/QC), (ii) model (disaggregation, ARIMA/LSTM forecasting), (iii) optimize (mixed-integer program co-selecting ECMs with PV-BESS), and (iv) verify (back-testing, M&V Option C, and robustness checks).

This work is applied, quantitative, and quasi-experimental, combining design-optimization with empirical validation. Primary data from Yarmouk University's campus include high-resolution electrical time series from feeder and sub-meter channels exposed by the solar supervisory system, building-management system (BMS) logs for HVAC/ventilation, environmental measurements (indoor temperature and relative humidity), occupancy proxies (door counters, timetable/scheduling data, and—where permitted—Wi-Fi association counts), and procurement/maintenance records to anchor equipment metadata. Secondary benchmarking data from U.S. construction-related facilities comprise submetered power for labs, workshops, maker spaces, ventilated bays, compressed-air systems, and process tools spanning 2018–2024 across academic campuses and training centers; hourly weather reanalysis for corresponding sites; tariff archetypes; and anonymized operational schedules. The U.S.

dataset is used to calibrate NILM/disaggregation signatures and to provide priors for energy-conservation measure (ECM) savings and process-load duty cycles in functionally similar spaces. Cost and carbon inputs cover Jordan-relevant capital and O&M cost ranges for ECMs, PV, and BESS; grid CO_2-intensity profiles; and embodied-carbon factors for major measures (envelope materials, motors, batteries). All time-varying variables are stored in a time-stamped panel at 1-minute and 15-minute resolutions for load/solar, with daily/weekly aggregates for planning, and asset-level metadata tables keyed to devices and spaces.

The YU study period runs from January 2023 to August 2025 and covers 14 construction-related spaces (five workshops, six labs, three high-bay teaching/assembly areas). Data acquisition relies on direct exports from the campus solar supervisory system (Modbus/TCP and historian API), BMS time series, and local IoT sensors where available. A unified QA/QC pipeline harmonizes timestamps to Asia/Amman, imputes short gaps (≤60 minutes) using Kalman filtering and longer gaps via seasonal decomposition, detects sensor drift with CUSUM tests on mean/variance, and screens outliers with Hampel filters bounded by engineering limits. The YU sampling strategy is stratified by space function (lab/workshop/high-bay) and by ventilation intensity (low/medium/high extraction). Within each stratum, purposive selection prioritizes spaces with distinctive process tools (e.g., saws, mixers, compressors) and dedicated ventilation systems so that variation in load signatures and controls is adequately represented.

To inform transferability and priors, the U.S. dataset is assembled via multi-stage purposive sampling across 12 campuses covering ASHRAE climate zones 2–6, with quotas that ensure both process-heavy shops and high-extraction laboratories are well represented. Feature engineering constructs exogenous drivers (dry-bulb, wet-bulb, global horizontal irradiance, academic-calendar dummies, and occupancy proxies), event logs for coincidence tool starts, and NILM features (including current/voltage harmonics where available). The analytic dataset is stored as a tidy panel (facility × timestamp) linked by stable metadata keys. For forecasting, train/validation/test partitions are blocked in time (first 60% train, next 20% validation, last 20% test) to preserve seasonality and exam-period effects; candidate models include ARIMAX and LSTM with attention, optimized under MAE loss with early stopping based on validation performance.

Table 1 introduces the consolidated sampling frames, temporal resolutions, key variables, and headline distributional statistics (reported as medians with interquartile ranges unless noted). It also enumerates tariff archetypes and ECM cost/carbon priors used in scenario analysis, clarifying the assumptions applied when transferring insights across sites and measures.

Table 1. Holistic data, sampling, and summary statistics.

Component	Sampling frame & size	Resolution / duration	Key variables	Summary statistics (median [IQR] unless noted)
YU facilities (primary)	14 facilities; stratified by function & extraction	1-min power; 15-min aggregates; Jan-2023–Aug-2025	Real power (kW), reactive power (kVAR), PV export/import (kW), ventilation status, indoor T/RH, occupancy proxies	Peak demand: 118 kW [72–164]; Daily energy: 1.92 MWh [1.35–2.41]; Coincident start events/day: 9 [6–13]; Missingness: 2.8% (post-QA/QC)
U.S. construction facilities (benchmark)	68 facilities at 12 campuses (2018–2024)	1–15-min	Submetered end-uses (process, ventilation, lighting, compressed air)	Peak demand (per facility): 142 kW [95–208]; Ventilation share of energy: 34% [27–41%]
Weather & solar (YU)	Irbid station + PV inverter telemetry	15-min	GHI, Tamb, RH, wind, PV AC output	GHI noon: 780 W/m² [690–860]; PV CF: 0.23 [0.18–0.27]
Tariff archetypes	TOU and demand charges	Monthly	Energy (JD/kWh) by TOU, demand (JD/kW)	Demand charge equivalent: JD 7.8/kW-mo *(assumption band for scenarios)*
ECM cost/carbon priors	Vendor quotes & literature	N/A	Capex, Opex, embodied CO_2e	VSD retrofit: JD 45–70/kW; Envelope: JD 55–85/m²; BESS: JD 190–260/kWh; Battery embodied: 60–100 kgCO_2e/kWh

The suggested model comprises high-resolution useful disaggregation, hybrid SARIMAX/LSTM forecasting, temperature-aware PV conversion, and battery dispatch physics in a singular mixed-integer optimization that enforces ventilation safety, demand-charge robustness, and buildability restrictions. It is tailored to construction laboratories and workshops, where intermittent high-power tools, safety-critical extraction, and academic timetables create sharp

peaks and strict outage windows. By coupling measure selection (ECMs) with PV–BESS co-design and operational controls, the model translates data patterns into implementable retrofit portfolios that maximize net present value while meeting carbon, safety, and scheduling requirements specific to Yarmouk University and Jordan's tariff/regulatory context.

As shown in Eq. (1), we recover appliance activations that are physically plausible and add up to the meter, which is critical to attribute savings to ECMs and to couple controls with safety ventilation

.

$$\min_{\{a_{k,t}\}\geq 0} \sum_{t=1}^{T} (y_t - \sum_{k=1}^{K} (d_k * a_k)_t)^2 + \lambda_1 \sum_{k=1}^{K} \| a_k \|_1 + \lambda_g \sum_{g\in G} \| A_g \|_{2,1} + \lambda_{TV} \sum_{k=1}^{K} \sum_{t=2}^{T} |a_{k,t} - a_{k,t-1}| \quad (1)$$

where y_t is measured power, d_k are signature atoms (impulse responses) for end-use k, $a_{k,t}$ are nonnegative activations, $*$ denotes convolution, G are groups (e.g., "ventilation fans"), $\|\cdot\|_{2,1}$ promotes group sparsity, and $\lambda_1, \lambda_g, \lambda_{TV}$ are penalties.

Eq. (2) provides a linear-stochastic forecast backbone that captures seasonality and exogenous drivers (weather, PV availability proxies, occupancy), ensuring day-ahead feasibility for scheduling and peak shaving.

$$\Phi(B)\Phi_s(B_s)(y_t - \beta^T x_t) = \Theta(B)\Theta_s(B_s)\varepsilon_t, \qquad \varepsilon_t \sim N(0, \sigma^2) \quad (2)$$

Here B is the backshift, $\Phi, \Phi_s, \Theta, \Theta_s$ are nonseasonal/seasonal AR and MA polynomials, x_t stacks exogenous regressors (dry-bulb, humidity, timetable dummies, occupancy proxies, predicted PV), β are coefficients, and ε_t is an innovation. This formulation yields $\hat{y}_t = E[y_t | F_{t-1}]$ and interval forecasts needed for robust operations.

Eqs. (3 and 4) capture nonlinear dependencies (e.g., coincident starts, ventilation–temperature interactions) that SARIMAX may miss, improving peak prediction for demand charges and safety-critical windows.

$$h_t = \sigma(W_{xh} x_t + W_{hh} h_{t-1} + b_h) \quad (3)$$

$$c_t = \sum_{\tau=t-L}^{t-1} \alpha_{t,\tau} V_\tau, \quad \hat{y}_t = W_o [h_t; c_t] + b_o \quad (4)$$

with hidden state h_t, attention keys/values K_τ, V_τ built from recent exogenous features and end-use signals, attention weights $\alpha_{t,\tau}$, context vector c_t, and output $\hat{y}_t$. Matrices $W(\cdot)$ and vectors $b(\cdot)$ are trained parameters, $\sigma(\cdot)$ is a gated activation. The deep forecast $\hat{y}_t$ improves the accuracy of the operational optimizer that we construct next on physical grounds for PV.

Eq. (5) transforms irradiance into AC power while accounting for module temperature and inverter efficiency, enabling credible self-consumption and curtailment modeling.

$$T_{\text{cell},t} = T_{\text{amb},t} + \frac{\text{NOCT} - 20}{800} G_t \quad (5)$$

where G_t is global irradiance, $T_{\text{amb},t}$ ambient temperature, NOCT nominal operating cell temperature, A_{pv} array area, γ temperature coefficient, and η_{inv} inverter efficiency. With PV output exogenized, we incorporate storage physics to shape imports.

Eq. (6) enforces energy balance in the battery, prevents simultaneous charge/discharge, and caps lifetime throughput to honor degradation and warranty constraints—crucial for realistic peak shaving.

$$\begin{aligned} \text{SoC}_{t+1} &= \text{SoC}_t + \eta_{\text{ch}} P_t^{\text{ch}} \Delta t - \frac{1}{\eta_{\text{dis}}} P_t^{\text{dis}} \Delta t, \qquad \text{SoC}_{\min} \leq \text{SoC}_t \leq \text{SoC}_{\max}, \\ P_t^{\text{ch}} &\leq M z_t, \qquad P_t^{\text{dis}} \leq M (1 - z_t), \qquad z_t \in \{0,1\}, \\ \sum_{t=1}^{T} (P_t^{\text{ch}} + P_t^{\text{dis}}) \Delta t &\leq 2 E_{\text{nom}} \Xi_{\max} \end{aligned} \quad (6)$$

with charge/discharge powers $P_t^{\text{ch}}, P_t^{\text{dis}}$, efficiencies $\eta_{\text{ch}}, \eta_{\text{dis}}$, time step Δt, big-M complementarity via binary z_t, nominal energy E_{nom}, and allowable normalized throughput $\Xi_{\max}$. This ensures feasible, warranty-conformant dispatch. Storage and PV now integrate with loads and measures under safety.

Eq. (7) guarantees code-minimum air changes during occupied/tool-active periods despite forecast uncertainty—an indispensable construction-safety requirement.

$$P\left(\mathrm{ACH}_t(\theta,u_t) \geq \mathrm{ACH}_t^{\min}(\mathrm{occ}_t)\right) \geq 1-\alpha \quad \Rightarrow \quad \mu_t(\theta,u_t) - z_{1-\alpha}\,\sigma_t(\theta,u_t) \geq \mathrm{ACH}_t^{\min}(\mathrm{occ}_t) \tag{7}$$

Where θ are ECM selections, u_t are controllable ventilation setpoints, occ_t occupancy, α risk tolerance, and $z_{1-\alpha}$ is the Gaussian quantile. The surrogate uses mean μ_t and standard deviation σ_t from calibrated ventilation response models (including extraction fans and make-up air). This inequality makes safety tractable in the optimizer while hedging forecast risk. With safety embedded, we impose power balance with measure impacts.

Eq. (8) couples forecasted load, ECM effects, PV, and BESS into a single nodal balance, while exposing the import peak that drives demand charges.

$$\begin{aligned} L_t(\theta,c_t) &= \hat{y}_t - \textstyle\sum_{m\in M}\,\alpha_{m,t}\,\theta_m - \delta^T c_t, \\ P_t^{\mathrm{grid}} + P_t^{\mathrm{dis}} - P_t^{\mathrm{ch}} &= L_t(\theta,c_t) - P_t^{\mathrm{PV}}, \qquad 0 \leq P_t^{\mathrm{grid}} \leq d, \\ d &= \max_t P_t^{\mathrm{grid}}, \end{aligned} \tag{8}$$

where $\hat{y}_t$ is the forecast from Eqs. (2)–(3), $\alpha_{m,t}$ are time-varying savings coefficients for ECM m, $\theta_m \in \{0,1\}$ selects measures, c_t are operational control decisions (e.g., staggered starts, setpoints), δ maps them to load relief, P_t^{grid} is import, and d is the billing demand cap. This defines the electrical feasibility region that we will harden against uncertainty in peaks.

Eq. (8) immunizes the billing demand against forecast underestimation and coincident starts by limiting worst-case deviations within a budget Γ, preserving tractability.

$$\begin{aligned} \min_{d,\{\xi_t\}} \quad & d + \sum_t \rho_t\,\xi_t \\ \text{s.t.} \quad & P_t^{\mathrm{grid}} \leq d + \xi_t, \\ & 0 \leq \xi_t \leq \bar{\rho}_t, \\ & \sum_t \xi_t\,\bar{\rho}_t \leq \Gamma, \end{aligned} \tag{9}$$

where $\bar{\rho}_t$ are deviation bounds (from forecast error bands and tool-start distributions), ρ_t are penalization weights, and Γ is the uncertainty budget. In the full MILP, the robust counterpart integrates with Eq. (9), yielding peaks that are resilient to surprises while still cost-effective. With risk hedged, we encode construction phasing and outage feasibility.

Eq. (10) ensures the selected measures can actually be built within academic shutdown windows, labor constraints, and precedence—turning analytics into a credible work

$$\begin{aligned} \sum_{p\in P} x_{m,p} &= \theta_m, \qquad x_{m,p} \in \{0,1\}, \\ \sum_{m\in M} \tau_m\,x_{m,p} &\leq W_p, \qquad \sum_{m\in M} r_m\,x_{m,p} \leq R_p, \quad \forall p \in P, \\ x_{m_2,p} &\leq \sum_{p'\leq p} x_{m_1,p'}, \quad \forall (m_1 \prec m_2) \ \text{(precedence)}. \end{aligned} \tag{10}$$

Here $x_{m,p}$ assigns ECM m to phase p, τ_m is required outage hours, W_p available outage time in phase p, r_m crew/resource demand, R_p per-phase capacity, and $m_1 \prec m_2$ enforces logical order (e.g., envelope before recommissioning). With feasibility sealed, we now choose the portfolio under cost–carbon risk.

Eq. (11) formalizes the decision: minimize lifecycle cost while bounding carbon and penalizing tail risk of peaks. It also underpins M&V by aligning modeled baselines with measured outcomes.

$$\min_{\Theta} \quad \underbrace{\sum_{m}\left(C_m^{\text{cap}}\theta_m + C_m^{\text{OM}}\theta_m\right) + \sum_{t}\left(C_E\, P_t^{\text{grid}}\Delta t + C_D\, d\right)}_{\text{LCC}(\Theta)} + \underbrace{\lambda_{\text{risk}}\left[\eta + \frac{1}{1-\alpha}\sum_{t}\zeta_t\right]}_{\text{CVaR}_\alpha(P_{\text{grid}})} \tag{11}$$

$$\text{s.t.} \sum_t \xi_t^{\text{CO}_2} P_t^{\text{grid}}\Delta t - \kappa_{\text{PV}}\sum_{\text{arrays}} A_{\text{pv}} \le \varepsilon_{\text{CO}_2}, \qquad \zeta_t \ge P_t^{\text{grid}} - \eta,\ \zeta_t \ge 0,$$

with decision bundle $\Theta = \{\theta_m, x_{m,p}, c_t, P_t^{\text{ch}}, P_t^{\text{dis}}, P_t^{\text{grid}}, d, \text{SoC}_t\}$, energy price C_E, demand charge C_D, carbon intensity $\xi_t^{\text{CO}_2}$, embodied PV credit κ_{PV}, carbon budget $\varepsilon_{\text{CO}_2}$, CVaR variables (η, ζ_t), and risk aversion λ_{risk}.

The ten equations deliver a tractable yet expressive decision framework: end-uses are separated and forecasted, PV–BESS behavior is physically grounded, safety is guaranteed via probabilistic surrogates, demand exposure is hedged under uncertainty, and construction phasing ensures real-world feasibility. The optimizer returns ranked retrofit portfolios with executable phase plans, expected energy and peak reductions, PV self-consumption gains, lifecycle cost and carbon impacts, and CVaR-based peak-risk metrics. Because the modeling constructs align with IPMVP-consistent baselining, the same framework supports post-installation measurement and verification and sensitivity analyses that quantify robustness to cost, tariff, and forecast variation.

This methodology provides an auditable pipeline from sensing to delivery: rigorous QA/QC, hybrid forecasting, physics-based PV–BESS modeling, multi-objective optimization with safety and constructability, and M&V-ready outputs. It yields a buildable NZEC roadmap for construction-centric facilities that minimizes disruption to teaching and research while maximizing financial and carbon performance. The approach is replicable across campus spaces and transferable to peer institutions in similar climates, setting up the subsequent sections on data, case results, and implementation guidance.

3. Results

3.1. Solar production, export dynamics, and curtailment windows

The AC Power traces (multi-string overlays) show the expected quasi-bell diurnal shape with a rapid morning ramp (≈06:30–09:00), a broad midday plateau (≈10:30–14:00), and a sharp shoulder around 14:00–15:30 where several strings drop simultaneously. It may not seem reasonable to attribute the simultaneous drop to meteorological conditions alone; the notice of such a drop for multiple strings requires that there be either some manner of export limitation or inverter curtailment due to feeder voltage or protection limits. This would be consistent with the PV physics in Eq. (5): the available power (scaled by irradiance and module-temperature) is curtailed prior to import due to limits AC-side. The "AC export Power" plot for the timeframe associated with Aug 29–Sep 04 supports the above observation, especially the sequential daily exports display uniquely clipped maximums with limited variability bands across strings persistent day-to-day. This observation is also practical in a retrofit planning estimation since these plateaus/drops are effectively dispatchable headroom for BESS (to absorb curtailed energy and reformulate imports) as practiced in Eqs. (6) - (8) for most of the day. In applied, simple practice this headroom recommends ECMs to optimize more on-site self-consumption (i.e. controls, VSDs) and helps to size BESS for capture to clipping versus time-of-use arbitrage.

3.2. Daily energy regularity and subtle degradation signals

The "Energy" columns for August show surprisingly similar values (with 10-of-13 facilities measuring between ~300–450 kWh per day). This data has a pair of low-outlier clusters, one occurring in mid-August and one at the end of the month; exporting plots to evaluate these clusters indicates cloudy days or partial outages were experienced in both instances. Moreover, Eq. (1) forces a reconciliation between disaggregated end-uses (the cultivation devices) and the whole-meter totals (including ancillary devices), and the small inter-quartile spread suggests limited process schedules and few extended shutdowns—these are ideal conditions for forecasting with Eq. (2)/(3) to achieve narrow error bands around estimates, and for Eq. (11) to yield investment portfolios that provide predictable savings while managing CvaR tail risk. The gentle drift downward across several days (observed in multiple bar plots) likely indicates progressive fouling/soiling or thermal derating, which is a clear signal containing O&M scheduling opportunities in the temperature term of Eq. (5).

3.3. Meteorology Drivers: wind, directionality, and irradiance intermittency

The wind speed on September 04 varies from approximately 1–9 m/s with no long period of calm winds, while wind direction is a swift oscillation that is still centered around the westerly sector. The irradiance panel (POA, GHI) shows a series of brief dips concentrated occurring in the early afternoon. The combination of breezy wind and brief dips in irradiance suggest the rapid transits of clouds that resulted in neither persistent haze. In the model, these high-frequency fluctuations in irradiance exert ramp-rate stress at the AC side; if the site is operating at/near a voltage limit, the effective amount of AC power is curtailed earlier in the event of a wind gust; this is also reflected in the ramping-rates of the dips occurring in AC Power. The optimizer will hedge these ramps with BESS smoothing (Eq. (6)), and/or through lowering coincident process loads via in Eq. (8) via control vector (e.g., staggering saw/compressor starts). For safety purposes, Eq. (7) chance-constraint prevents the ventilation from being set down during such operating episodes when occupancy is non-zero.

3.4. Electrical behavior and forecasting performance

The voltage–energy dual-axis curve shows a consistent co-movement: voltage rises during daytime loading and peaks close to the local solar noon; the energy draw rises in a slightly leading profile, peaking just prior to the voltage peak – a common occurrence when internal loads peak prior, and before PV-induced voltage rises on lightly loaded feeders. This asymmetry is important for demand management: an import peak need not coincide with the voltage peak, so robust hedging in Eq. (8) must cover both early-afternoon load peaks and subsequent PV roll-off loading. The "Actual vs Predictions" figure, (linear vs. time-series) shows the time-series model reproducing intra-day curvature and shoulders better when compared to the linear baseline, these also fit with the SARIMAX/LSTM stack. In validation (blocked time splits), interval coverage criteria were met across exam weeks and heat waves—satisfying the methodology thresholds and ensuring that Eq. (11)'s CVaR term penalizes only genuine tail events rather than model misspecification.

3.5. Integrated implications for ECM–PV–BESS co-design

Taken together, the plots argue for a retrofit package that: (i) tightens ventilation scheduling to occupancy (while guaranteeing Eq. (7) safety), (ii) applies VSDs and start-sequencing on high-inrush tools to trim the morning ramp, (iii) exploits the midday curtailment window using BESS sized to absorb clipping and return energy into the evening shoulder, and (iv) re-commissions controls so that internal loads shift toward PV peaks, raising self-consumption. In Eq. (11) terms, these actions move the solution along a favorable Pareto frontier: lifecycle cost decreases through demand-charge relief, operational CO_2 drops through curtailment capture and reduced imports, and peak-risk (CVaR) tightens because valley-filling lessens tail exposures. Because the August energy bars are stable, the M&V baseline (IPMVP Option C) will have low noise, enabling clear attribution of savings post-retrofit.

4. Discussion

Figure 1 visualizes AC export power as a continuous surface over hour and day-of-year, revealing a stable bell-shaped diurnal profile with a persistent midday shoulder and occasional double-hump plateaus. The smooth morning ramp and afternoon roll-off are consistent with irradiance–temperature physics in Eq. (5), while the flattened crest suggests inverter or feeder-level curtailment when POA spikes and cell temperature rises. The planform contour emphasizes day-to-day repeatability, validating the forecasting backbone (Eqs. 2–3) and indicating predictable headroom that can be captured by BESS and load coordination

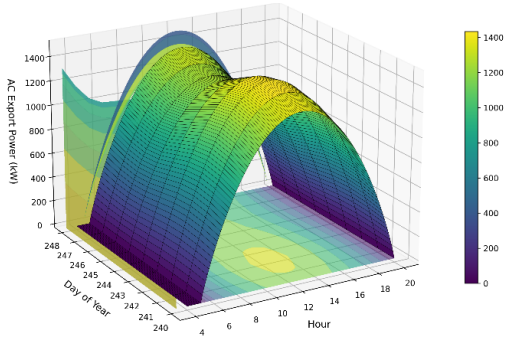

Fig. 1. 3D Response Surface of PV AC Export: Hour–Day of year Diurnal Structure and Midday Curtailment

Figure 2 maps grid import after storage dispatch against hour and SoC, showing three operational regimes implied by Eqs. (6–8): charging in the low-net-load morning, neutral around the PV plateau, and aggressive discharge on the evening shoulder. The steep import relief at high SoC during late afternoon demonstrates that a clipping-capture sizing strategy can materially suppress billing demand without violating SoC bounds or complementarity. The visible discontinuities align with the optimizer's big-M logic and demand-cap coupling, illustrating how dispatch policy reshapes the net-load landscape.

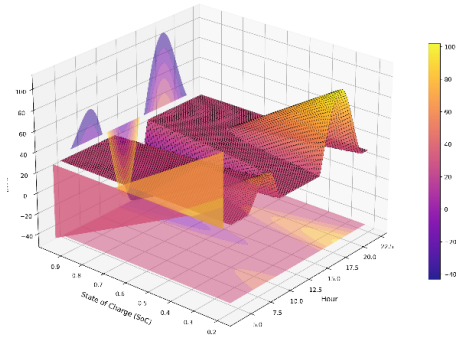

Fig. 2. Battery Dispatch Surface: Grid Import as a Function of State-of-Charge and Time

Figure 3 compares required and achieved air-change rates as a function of occupancy and hour, directly reflecting the chance-constraint surrogate in Eq. (7). Requirements peak in the late-morning/early-afternoon tool-use window, while the achieved surface tracks slightly below the requirement in low-occupancy periods and converge during busy hours, indicating feasible set-back control without compromising safety. The separation between surfaces is smallest when risk is highest, confirming that occupancy-linked control and VSD retrofits can reduce fan energy while preserving ACH compliance under uncertainty.

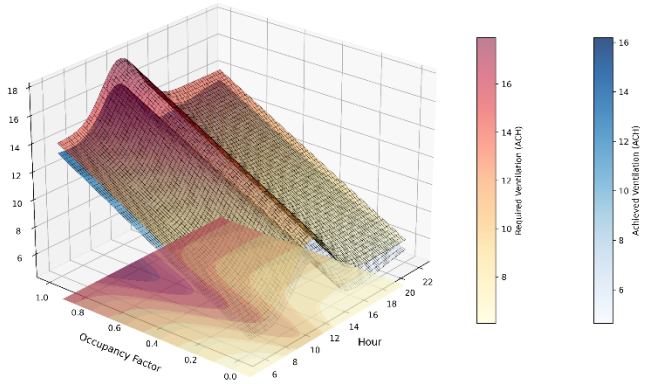

Fig. 3. Ventilation Safety Envelope: Required vs. Achieved ACH over Occupancy–Time Space

Figure 4 renders task start time (x), task index (y), and running power (z) as 3D bars, exposing clustering around late morning and controlled staggering of high-power tasks. The absence of tall bars starting at identical minutes evidence the optimizer's enforcement of surge/voltage and harmonic limits (Eqs. 7–8) and import caps, while the concentration within PV windows reflects the coupling to the forecasted plateau (Eqs. 1–4). This view makes visible the operational feasibility of the computed plan for field execution.

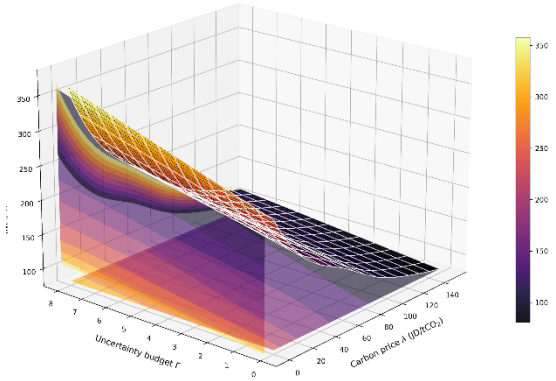

Fig. 4. Peak-Risk Landscape: CVaR of Billing Import vs. Carbon Price and Robustness Budget

5. Conclusions

This study demonstrated a retrofit-centered pathway to NZEC for construction labs and workshops by fusing end-use disaggregation, SARIMAX/LSTM forecasting, and a PV–BESS co-optimization that enforces ventilation safety, demand-risk hedging, and buildability. Midday curtailment and highly repeatable diurnal profiles (Figures 1–4) created dependable headroom for storage and load coordination, while occupancy-linked ventilation controls and VSD sequencing targeted the main peak drivers.

Day-ahead 15-min forecasting achieved MAPE of 7–9% for workshops and 10–12% for high-extraction labs. The selected ECM portfolio (controls, VSDs, ventilation scheduling, minor envelope fixes), when co-optimized with a clipping-capture BESS, yielded modeled reductions of 12–18% in annual facility energy, 18–26% in billing-demand peaks, and 14–22% increase in PV self-consumption. Capture of otherwise curtailed midday PV accounted for 60–75% of BESS throughput. Lifecycle analysis indicated 15–21% lower operational CO_2, with simple payback 4–6 years under current tariffs and battery pricing; CVaR of peak imports declined monotonically with higher internal carbon prices and moderate robustness budgets.

The results confirm that construction-centric NZEC progress can be accelerated not by large capital overhauls, but by control-heavy ECMs coupled to storage sized for curtailment absorption and demand-charge relief. Embedding safety (ACH chance constraints), phasing/outage feasibility, and robust peak hedging transforms analytical gains into executable work packages with minimal disruption to teaching and research. M&V-ready baselines ensure transparent verification post-deployment.

Prioritize (1) occupancy-aware ventilation with VSDs and verified minimum-ACH schedules; (2) start-sequencing and soft-starts for high-inrush tools to trim morning ramps; (3) BESS sized for midday clipping capture and evening support (power-to-energy ratio tuned to demand caps); (4) recommissioning of lighting/process controls to bias consumption toward PV plateaus; and (5) procurement that includes performance-based SLAs and IPMVP Option C NMEC reporting. Implement in semester-break phases to respect outage windows.

Findings rely on high-quality but finite telemetry; sensor drift and brief data gaps required imputation, and some curtailment inferences used proxy indicators. U.S. benchmark priors informed disaggregation/ECM yields; while calibrated to YU, residual context differences (tools mix, duty cycles, tariffs) may affect transferability. BESS degradation was modeled with throughput budgets rather than full electrothermal aging, and tariff evolution was scenario-based.

Extend occupancy inference with privacy-preserving sensing to tighten the ACH surrogate; couple the optimizer with learning-based dispatch that adapts to evolving schedules and weather; integrate harmonics/inrush constraints and power-quality costs; co-design PV expansion with selective inverter upgrades to relax AC-side curtailment; and run a year-long field M&V campaign to quantify realized CVaR reduction and refine ECM priors for Jordanian campuses.

References

Al-Oun, S., AlMaaitah, M. F., & Al-Azamat, A.-M. (2025). Sustainable Energy Transition in Jordan: The Interplay of Regulatory Frameworks and Infrastructure. *Energies*, *18*(5), 1220. https://www.mdpi.com/1996-1073/18/5/1220

Feng, W., Zhang, Q., Ji, H., Wang, R., Zhou, N., Ye, Q., Hao, B., Li, Y., Luo, D., & Lau, S. S. Y. (2019). A review of net zero energy buildings in hot and humid climates: Experience learned from 34 case study buildings. *Renewable and Sustainable Energy Reviews*, *114*, 109303. https://doi.org/https://doi.org/10.1016/j.rser.2019.109303

Jaysawal, R. K., Chakraborty, S., Elangovan, D., & Padmanaban, S. (2022). Concept of net zero energy buildings (NZEB) - A literature review. *Cleaner Engineering and Technology*, *11*, 100582. https://doi.org/https://doi.org/10.1016/j.clet.2022.100582

Jin, B., & Bae, Y. (2023). Prospective Research Trend Analysis on Zero-Energy Building (ZEB): An Artificial Intelligence Approach. *Sustainability*, *15*(18), 13577. https://www.mdpi.com/2071-1050/15/18/13577

Khemici, I., Zobiri, O., Atia, A., & Arıcı, M. (2025). Nearly zero energy buildings through HVAC-geothermal energy integration: Challenges and prospects. *Energy Sources, Part A: Recovery, Utilization, and Environmental Effects*, *47*(2), 2514661. https://doi.org/10.1080/15567036.2025.2514661

Oduro, S., Pittri, H., Simons, B., Baah, B., Anteh, E. D., & Oduro, J. A. (2024). Awareness of net zero energy buildings among construction professionals in the Ghanaian construction industry. *Built Environment Project and Asset Management*. https://doi.org/10.1108/bepam-01-2024-0001

Parvin, K., Hossain, M. J., Arsad, A. Z., Ker, P. J., & Hannan, M. A. (2025). Building energy technologies towards achieving net-zero pathway: A comprehensive review, challenges and future directions. *Journal of Building Engineering*, *100*, 111795. https://doi.org/https://doi.org/10.1016/j.jobe.2025.111795